This article has been accepted for publication in a future issue of this journal, but has not been fully edited. Content may change prior to final publication. Citation information: DOI 10.1109/TSTE.2017.2697913, IEEE Transactions on Sustainable Energy

Estimation of Solar Irradiance on Solar Fields: an Analytical Approach and Experimental Results

Samer Yassin Alsadi, *Member, IEEE* and Yasser Fathi Nassar

***Abstract*—An extensive experiment has been designed and conducted to measure the magnitude of solar irradiance falling upon a PV solar field. The experimental results show that the second and succeeding rows received less solar irradiance than the first row. In addition, there was a degradation of the solar irradiance along a single row directing towards the centre of that row. Nowadays, all available models are addressing the solar radiation incident on a single surface. However, the nature of multi-rows solar fields is different from that of a single surface, which indicates that these models are not suitable for solar irradiance calculation, and there is no work regarding this topic. The aim of this study is to modify a model so the design parameters are included in one model that estimates the solar irradiance on solar fields. The effect of the design parameters, was demonstrated. In order to state the validity of the proposed model, a comparison between models that were used in literature and the proposed model along with the experimental results has been provided. The impact of solar degradation on the electrical characteristics has been briefly discussed.**

***Index Terms*—Solar irradiance on solar field, sky view factor, ground view factor, rear surface view factor, shaded zone, illuminated zone, solar field design parameters, isotropic sky model.**

I. Introduction

IT is widely accepted that photovoltaic (PV) solar energy is an abundant, a clean, and a secure source of electricity. According to Global Data's latest report, the global installed capacity of solar PV will increase from 271.4 GW in 2016 at a compound annual growth rate of 13.1% to 756.1 GW in 2025. Libya is not excluded from this scene, because of the initial steps that the Libyan government is considering in order to put forward developmental plans to construct several PV power plants in different locations: in Derna (east of the country) with the capacity of 60 MW; Al-Jufrah (centre of the country) with the capacity of 15 MW, in Sebha (south of the country) with the capacity of 40 MW, and in Gdames (west of the country) with the capacity of 200 MW.

Models and softwares developed and utilized by researchers to estimate solar irradiance and PV-array performance in solar fields are listed in [1]. Most of these models give users one or more options for solar irradiance on a tilted surface and include: 1) Isotropic sky, 2) Temps and Coulson (1977), 3) Bugler (1977), 4) Klucher (1978), 5) Hay & Davies (1979), 6) Willmott (1982), 7) Skartveit & Olseth (1986), 8) Gueymard (1987), 9) Perez (1988), 10) Reindl (1990). Moreover, modelling the solar irradiance in solar fields involves two steps: 1) The decomposition of global horizontal irradiance (G) into its direct and diffuse components, usually expressed as diffuse horizontal irradiance (G_d) and direct beam irradiance (G_b), and 2) The transposition of these components to solar irradiance of the modules [2]. All decomposition models effectively produce estimates of both (G_d) and (G_b), and they are well documented in all textbooks of solar energy, such as, Duffie and Beckman [3], and Nassar [4]. While, the transposition models determine total solar irradiance in solar fields by estimating the direct, ground-reflected and sky-diffuse components on the solar field. The required data for transposition models is tabulated in table (1).

Table 1
The requirements for transposition models [2]

Model	Input variables
Isotropic	S, G_b, G_d
Sandia	S, G_b , G_d , α
Hay/Davies	S, G_b , G_d , H_o, θ_z
Perez	S,, G_b , G_d , H_o, θ_i, θ_z, AM

where H_o is the extraterrestrial radiation flux and AM is the air mass. The isotropic, Hay&Davies, Reindl and Perez models are the most commonly used transposition models. The Sandia model is identical to the isotropic model, except that it uses an empirically derived ground albedo instead of assuming a constant value. The transposition models determine total solar irradiance (G_T) on solar fields by estimating the direct ground-reflected and sky-diffuse components are isotropic on the solar field [5]:

$$G_T = \left[G_b R_b + G_d \frac{(1+\cos S)}{2} + G\varrho_g \frac{(1-\cos S)}{2}\right] \qquad (1)$$

In Eq. (1), $\varrho_g = 0.2$ is the ground albedo, S is the slope of the panel, and R_b is the ratio of beam radiation on a tilted surface to that on a horizontal surface. All transposition models use eqn.(1). The Isotropic, Hay&Davies, and Perez models use a constant albedo. The Sandia transposition model uses an albedo equation that was empirically fit to data from Albuquerque, NM, USA [2]:

$$\varrho_g = 0.012 \times \theta_z - 0.04 \qquad (2)$$

where θ_z is the solar zenith angle in degrees. The transposition models vary in their estimation of the sky-diffuse irradiance (G_d) on the solar field. The Isotropic and Sandia models use an isotropic sky assumption such that the diffuse irradiance on solar field depends only on the amount of sky "seen" by the surface. The National Renewable Energy Laboratory System Advisor Model (SAM) is used four radiation models included in the TRNSYS radiation processor within SAM: Perez, Hay & Davies, Reindl, and isotropic sky [6,7]. While in the EnergyPro is used the Reindl model [8].

However, the amount of diffuse radiation on the row depends on the view factors of the row to sky and the sky irradiance distribution. The amount of the reflected radiation from the ground and preceding row depends on the view factors of the ground and the rear surface of the preceding row. The view factors vary with the design parameters of solar fields (S, ψ, L_c, H_c, X) and hence, the diffuse and reflected incident radiation on solar cells in different rows (strips) of the PV panel vary, resulting in current mismatch between cells in the different rows [9-11]. Furthermore, shadowing effects even the collector are assumed to be illuminated from the ground in front of the row will be partially shaded, this will affect in the ground-reflected irradiance value [11]. In additional, there is a fourth component involved in the total solar irradiance that is the reflected irradiance from the rear surface of the preceding

This article has been accepted for publication in a future issue of this journal, but has not been fully edited. Content may change prior to final publication. Citation information: DOI 10.1109/TSTE.2017.2697913, IEEE Transactions on Sustainable Energy

row. All the above mentioned models do not include the most important parameter in solar field design which is the space separating the rows (X), as one recognised from table (1). The questions are raising now: How one can we assess the influence of the design parameters of a solar field on the performance and profitability of the solar energy?, and What should we do if the solar field is not a flat-field?

According to what has been presented in literature reviews, it can be briefly summed up that deficiencies in the mathematical models are used to estimate the solar irradiance on solar fields in the following points:

1. The view factor between the second and succeeding rows and the sky so far is not $\frac{(1+\cos S)}{2}$;
2. The view factor between the second and succeeding rows and the ground so far is not $\frac{(1-\cos S)}{2}$;
3. The ground-reflected solar irradiation G is not always equal to the sum of the beam and sky-diffuse radiation due to the shadow of the preceding row on the ground-space that separates the rows.
4. The design parameters and type of the solar field are not included.
5. A fourth term is missing in these models, which is the reflected irradiance from the rear-surface of the preceding row.

According to what is mentioned on the literature review, the discussion of the subject in this perspective is unprecedented, and its accomplishment is a significant contribution to the field of solar energy.

In order to prove reality of the study and to state the validity of the proposed model, an experiment has been conducted to measure the amount of solar irradiance incident on the second row of a prototype solar field built in Engineering Faculty, Brack-Libya.

The approach presented below calculates the solar irradiance on a solar field, and thus enables us to assess the influence of the design parameters on the performance and profitability of the solar field. The presented model in this work is comprehensive and generally able to consider any other configuration of arrangements, such as: inclined plane or step-like structure solar fields, and roofs or facades of buildings; it only requires identifying the view factors between collectors and environments. Furthermore, the proposed approach makes it possible to estimate (hourly, daily, monthly, and annually) solar irradiation incident on a solar field and visualize the prospects of augmentation of solar energy. Despite the relative complexity of the analysis, the model can be easily implemented, and it could be developed as a software for widely use.

II. Total Irradiance on a Single Tilted Surface

There are many well-known methods of obtaining the irradiance on a single surface. The best way, however, is to measure the irradiance on a horizontal or tilted plane, and for the additional calculations, it is necessary to estimate not only the global irradiance. If the measurements of the global irradiance are only available, it is possible then to split up the global irradiance into direct and diffuse irradiance with statistical correlations [2].

The approach considers the isotropic model, and includes components of beam (I_b), diffuse (I_d) irradiation and irradiation reflected from the ground (I_r). The total solar radiation (I_t) on a tilted surface at slope (S) from the horizontal for an hour as the sum of three components is given as:

$$I_t = I_b R_b + I_d F_{A1\to s} + I_r \varrho_g F_{A1\to g} \ , \quad \left[\frac{W}{m^2}\right] \qquad (3)$$

Where I_b is the hourly beam radiation from the sun on a horizontal surface, I_d is the hourly diffuse irradiation I_r is the hourly ground-reflected irradiation $I_r = I_b + I_d$. The beam and sky diffuse irradiance may be obtained from the metrological stations or calculated by using the analytical models. In this research, we used the ASHRAE clear sky model for calculating beam and sky-diffuse irradiance. The constants of the ASHRAE model had been corrected by Alsadi and Nassar (2016) for many locations [12].

The geometric factor R_b:

$$R_b = \frac{\cos(\theta_i)}{\cos(\theta_z)} \qquad (4)$$

And:

$F_{A1\to s}$, is the view factor of the surface to the sky;
$F_{A1\to g}$, is the view factor of the surface to the ground;
ϱ_g, is the ground albedo;
θ_i, is the incident angle;
θ_z, is the solar zenith angle

$$\theta_i = cos^{-1}[sinS\ cos\theta_z\ cos(\phi-\psi) + cosS\ sin\theta_z] \qquad (5)$$

ϕ, is the solar azimuth angle. Where:

$$\theta_z = cos^{-1}[sin\delta\ sinL + cos\delta\ cosL\ cosh] \qquad (6)$$

$$\phi = cos^{-1}\left[\frac{sin\delta\ cosL - cos\delta\ sinL\ cosh}{\sin\theta_z}\right] \qquad (7)$$

$$\delta = 23.45sin\left[\frac{360}{365}(n+284)\right] \qquad (8)$$

Where: L denotes the local latitude angle, δ is the declination angle, and h is the hour angle: $h = 15(t_s - 12)$ in where t_s presents the solar time, and n is the Julian day of the year starting from January 1.

The following are the expressions for the view factors of the sky-diffuse and the ground-reflected irradiance for a single tilted surface:

$$F_{A1\to s} = \frac{1+\cos(S)}{2}$$
$$F_{A1\to g} = \frac{1-\cos(S)}{2} \qquad (9)$$

III. Solar Irradiance on a Solar Field

The above mentioned solar radiation model is not generally able to consider all rows of the solar field since the second row faces neither the sky nor the ground in the same perspective as the first row. Therefore, the view factors in eqn. (9) must be modified.

The approach is based on the following assumptions:

1. The length of the row is very long with respect to the height ($L_c \gg H_c$).
2. The sky-diffuse radiation is considered to be isotropic.
3. The rear-surface of A_1 only receives sky-diffuse and ground-reflected solar irradiance;
4. The façade of the collector is always illuminated. The shadow has been avoided in order to focus on the change of solar irradiation intensity along the solar field.
5. All the dimensions are the same for all rows of the solar field (S, ψ, L_c, H_c, X).

Fig.1 represents a cross section of two rows of a solar field, where A_1 and A_2 present the surfaces of the first and the second row, respectively.

This article has been accepted for publication in a future issue of this journal, but has not been fully edited. Content may change prior to final publication. Citation information: DOI 10.1109/TSTE.2017.2697913, IEEE Transactions on Sustainable Energy

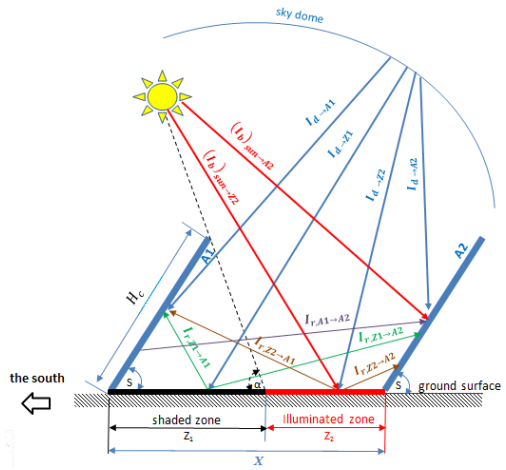

Fig.1. 2-D solar irradiation components and the shaded (Z_1) and the illuminated (Z_2) zones. Where: $(I_b)_{sun\to A2}$ and $(I_b)_{sun\to Z2}$ are the beam from the sun to the surface A_2 and the illuminated zone Z_2 respectively, $I_{d\to A2}$, $I_{d\to A1}$, $I_{d\to Z2}$ and $I_{d\to Z1}$ are the isotropic sky diffuse to the surface A_2, A_1, Z_2 and Z_1 respectively, $I_{r,Z2\to A2}$ and $I_{r,Z2\to A1}$ are the ground reflected components from the illuminated zone Z_2 toward the surface A_2 and the rear surface A_1 respectively, $I_{r,Z1\to A2}$ and $I_{r,Z1\to A1}$ are the ground reflected components from the shaded zone Z_1 toward the surface A_2 and the rear surface A_1 respectively, and $I_{r,A1\to A2}$ is the reflected irradiation from the rear surface A_1 toward A_2.

As illustrated in fig.1, the distance separating the rows (X) is almost partially shaded. Generally, this area includes two zones: one is shaded zone Z_1 and the other is illuminated zone Z_2. The expression has been derived and written as:

$$Z_1 = H_c\left[\cos(S) + \frac{\sin(S)}{\tan(\alpha)}\right] \quad \text{, and}$$
$$Z_2 = X - Z_1 \qquad (10)$$

The sun elevation angle (α) which at a given time is assumed a constant for the whole field is given by [3]:

$$\propto = sin^{-1}[\sin(\delta)\sin(L) + \cos(\delta)\cos(L)\cos(h)] \quad (11)$$

According to the above mentioned analysis, the definition of all irradiances that strike the surface A_2, as illustrated in fig.1, the total solar irradiance on the second row (I_f) may be expressed in the form of isotropic model as:

$$I_f = \begin{cases} [I_b \forall_2 R_{b2}] + [I_d F_{A2\to s}] + \\ \left[(I_b + I_d)\varrho_g \frac{Z_2}{H_c} F_{A2\to Z2} + I_d \varrho_g \frac{Z_1}{H_c} F_{A2\to Z1}\right] + \\ \left[\left(\begin{matrix} I_b \forall_1 R_{b1} + I_d F_{A1\to s} + I_d \varrho_g \frac{Z_1}{H_c} F_{A1\to Z1} + \\ (I_b + I_d)\varrho_g \frac{Z_2}{H_c} F_{A1\to Z2} \end{matrix}\right)\varrho_{A1} F_{A2\to A1}\right] \end{cases} \qquad (12)$$

Values of the beam (I_b) and diffuse (I_d) solar irradiance, which are mentioned in eqn. (12), are similar to those in eqn. (3), but the view factors are different from that of a single surface. The distance separating the rows may be partially shaded, which means that the shading area receives only sky-diffuse irradiance and not beam irradiance; while, the illuminated region receives both direct and sky-diffuse irradiance. In addition, the second row and the succeeding rows receive another irradiance which is reflected from the rear-surface of the preceding row. All the above mentioned explanations have to be taken into consideration when planning or simulating solar systems in solar fields.

In eqn. (12) the first square-bracket represents the direct beam, the second bracket represents the isotropic sky-diffuse irradiation. The third bracket represents the ground-reflected irradiation which is including two parts: the illuminated zone which is combined from both beams and diffuses, and the shaded zone includes only the isotropic diffuse only, and the fourth bracket indicates the irradiation that is reflected from the rear surface of the preceding row A_1 onto the collector surface A_2.

The area ratio factors $\forall_1$ and $\forall_2$ represent the ratio of the portion of the collector area as seen directly from the sun; therefore, the portion of the collector area which is not shadowed, for the rear surface of the collector A_1 and for the front surface of the collector A_2, respectively. According to our assumptions ($\forall_1 = 0$ and $\forall_2 = 1$).

$F_{A2\to s}$ is the view factor of the sky with respect to the front surface of the collector A_2 , therefore the second bracket of eqn. (12) represents the isotropic diffuse radiation component from the sky as seen by the collector A_2.

$F_{A2\to Z2}$ is the view factor of the ground-illuminated zone to the front surface of the collector A_2 , therefore the first term in the third bracket of eqn. (12) represents the reflected radiation component from the illuminated portion (Z_2) of the ground as seen by the collector A_2.

$F_{A2\to Z1}$ is the view factor of the ground-shaded zone to the front surface of the collector A_2 . Therefore, the second term in the third bracket of eqn. (12) represents the reflected radiation component from the shaded portion (Z_1) of the ground as seen by the collector A_2.

$F_{A1\to s}$ is the view factor of the sky with respect to the rear surface of the collector A_1 , therefore the second term in the fourth bracket of eqn. (12) represents the isotropic diffuse radiation component from the sky as seen by the back side of the collector A_1.

$F_{A1\to Z2}$ is the view factor of the ground-illuminated zone to the rear surface of the collector A_1 ; therefore, the fourth term in the fourth bracket of eqn. (12) represents the reflected radiation component from the illuminated portion (Z_2) of the ground as seen by the back side of the collector A_1.

$F_{A1\to Z1}$ is the view factor of the ground-shaded zone to the rear surface of the collector A_1 ; therefore, the third term in the fourth bracket of eqn. (12) represents the reflected radiation component from the shaded portion (Z_1) of the ground as seen by the back side of the collector A_1.

$F_{A2\to A1}$ is the view factor of the rear surface of the collector A_1 with respect to the front surface of the collector A_2, therefore, the fourth bracket of eqn. (12) represents the reflected radiation from the rear surface of collector A_1 as seen by the collector A_2.

Some of the view factors mentioned above have been derived by Nassar and Alsadi in [11]; the others are derived in this work. All the view factors will be presented in dimension less forms as:

$$F_{A2\to s} = 0.5\left[1 + \frac{X}{H_c} - \sqrt{(sin(S))^2 + \left(\frac{X}{H_c} - cos(S)\right)^2}\right] \qquad (13)$$

$$F_{A2\to Z2} = 0.5\left[1 + \frac{Z_2}{H_c} - \sqrt{(sin(S))^2 + \left(\frac{Z_2}{H_c} + cos(S)\right)^2}\right] \qquad (14)$$

$$F_{A2\to Z1} = 0.5\left[\frac{Z_1}{H_c} - \frac{\sqrt{(sin(S))^2 + \left(\frac{X}{H_c} + cos(S)\right)^2} + }{\sqrt{(sin(S))^2 + \left(\frac{Z_2}{H_c} + cos(S)\right)^2}}\right] \qquad (15)$$

This article has been accepted for publication in a future issue of this journal, but has not been fully edited. Content may change prior to final publication. Citation information: DOI 10.1109/TSTE.2017.2697913, IEEE Transactions on Sustainable Energy

$$F_{A2\to A1} = 0.5\left[-2\frac{X}{H_c} + \sqrt{(sin(S))^2 + \left(\frac{X}{H_c} - cos(S)\right)^2} + \sqrt{(sin(S))^2 + \left(\frac{X}{H_c} + cos(S)\right)^2}\right] \quad (16)$$

$$F_{A1\to s} = 0.5\left[1 + \frac{X}{H_c} - \sqrt{(sin(S))^2 + \left(\frac{X}{H_c} + cos(S)\right)^2}\right] \quad (17)$$

$$F_{A1\to Z1} = 0.5\left[1 + \frac{Z_1}{H_c} - \sqrt{(sin(S))^2 + \left(\frac{Z_1}{H_c} - cos(S)\right)^2}\right] \quad (18)$$

$$F_{A1\to Z2} = 0.5\left[\frac{Z_2}{H_c} - \sqrt{(sin(S))^2 + \left(\frac{X}{H_c} - cos(S)\right)^2} + \sqrt{(sin(S))^2 + \left(\frac{Z_1}{H_c} - cos(S)\right)^2}\right] \quad (19)$$

$$F_{A1\to A2} = 0.5\left[-2\frac{X}{H_c} + \sqrt{(sin(S))^2 + \left(\frac{X}{H_c} - cos(S)\right)^2} + \sqrt{(sin(S))^2 + \left(\frac{X}{H_c} + cos(S)\right)^2}\right] \quad (20)$$

IV. Results and Discussion

A. Analytical approach results

In order to achieve the goal of this study, an MsExcel sheet is prepared and proceeding all the equations that we have introduced above. Typical of the obtained results are demonstrated and discussed below.

Some of the view factors are constants; they depend on the solar field design parameters (S and $\frac{X}{H_c}$) only. These view factors are: $F_{A2\to s}$, $F_{A2\to A1}$, and $F_{A1\to s}$, whereas the rest of them are unsteady and depending on the time and location as well as the solar field design parameters.

The sky view factors ($F_{A1\to s}$) and ($F_{A2\to s}$) are slowly growing with increasing the ratio ($\frac{X}{H_c}$). In contrast, the view factor ($F_{A2\to A1}$) decreases slowly at low tilt angles when increasing ($\frac{X}{H_c}$) ratio and rapidly decays with high tilt angles especially in high latitudes in where apply high tilt angles. However, increasing the tilt angle results in increasing the values of ($F_{A1\to s}$) and ($F_{A2\to A1}$) while diminishing ($F_{A2\to s}$).

To calculate the unsteady view factors and the solar irradiance on solar fields, it is very important to determine the length of shadow Z_1. For this reason, a dimensionless parameter is created for the shaded zone: The Shadow length ratio $\left(\frac{Z_1}{X}\right)$ is calculated from eqn. (10) by dividing the both sides of the equation by X, so:

$$\frac{Z_1}{X} = \frac{\left[\cos(S) + \frac{\sin(S)}{\tan(\alpha)}\right]}{\frac{X}{H_c}} \quad (21)$$

This parameter presents the ratio between the shadow length and the distance separating the rows. This parameter is important for ground-view factor calculation. The dimensionless shadow length ratio ($\frac{Z_1}{X}$) is calculated and plotted in fig. 2.b at the solar-noon vs. the solar altitude angle (α) for various tilt surface angles (S) and for distance ratio ($\frac{X}{H_c} = 1$). The solar altitude angle has been calculated at the solar-noon and presented in fig.2.a, vs. time and location of interest. The benefit of fig. 2 that, it presents knowledge of shadow length at any day and for any location. For south facing solar field at solar-noon ($\phi = 0°$) and for specific solar altitude angle (α), the shadow length is longer in high latitudes. This trend decays until the ratio $\left(\frac{Z_1}{X}\right)$ is equal to one when $\alpha = \frac{180°-S}{2}$. The shadow vanishes when the sun is located on the extended plane of the collector ($\alpha = S$), and ($\phi = 180°$) for south facing collectors. The minus sign which appears in fig. 2.b for ($\alpha < S$) and ($\phi = 180°$) indicates that the sun is located behind the collector and the shadow becomes on the opposite direction of the abscissa x; the collector's façade is now fully shaded. At solar-noon, this situation may occur in sites which are located between Capricorn and Cancer tropics ($23.45°S < L < 23.45°N$), as it appears in fig.2.a. The solar altitude curves for latitude angles L= 0°,10° and 20°, show different behaviour from the others. This occurs because the sun arises from the forward (the first peak) and then sets from the backward (the second peak) of the collector.

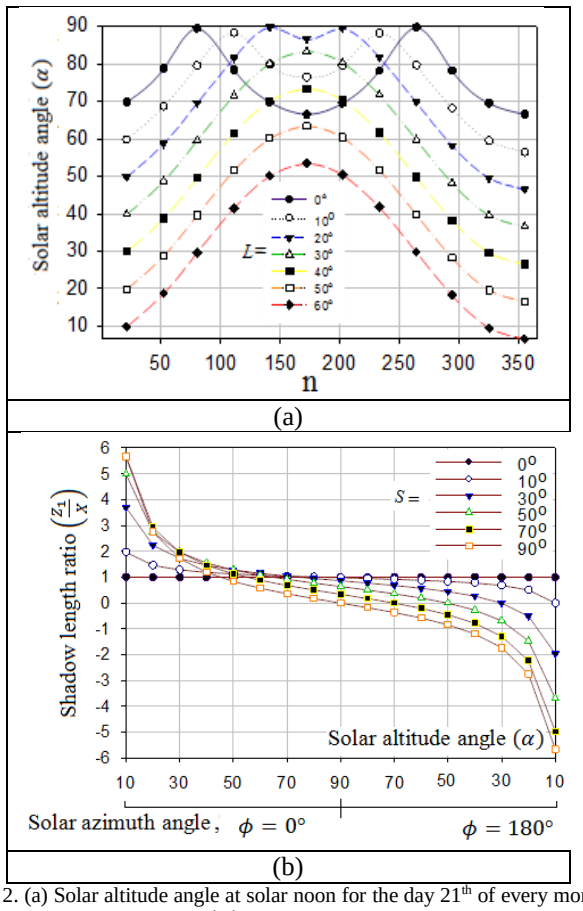

Fig. 2. (a) Solar altitude angle at solar noon for the day 21th of every month, and (b) Shadow length ratio $\left(\frac{Z_1}{X}\right)$ as a function of the solar altitude angle (α) for several surface tilt angles (S), and for south facing surface ($\psi = 0°$) at the solar-noon ($\phi = 0°$ or 180°), and the distance ratio ($\frac{X}{H_c} = 1$).

It must be mentioned that care should be considered when conducting simulation of such systems because we have to choose values for the variables that do not conflict with the research assumptions. We have assumed that, the solar collector is always illuminated. Accordingly, X must be at least not less than Z_1 at the design point (time and location). it is definitely not possible to avoid the shadow completely, since the shadow length is very long in the early morning and late evening and even relatively longer during winter solstice in the northern hemisphere. For this reason, we have depicted in fig.3 the relationship between the minimum distance ratio

This article has been accepted for publication in a future issue of this journal, but has not been fully edited. Content may change prior to final publication. Citation information: DOI 10.1109/TSTE.2017.2697913, IEEE Transactions on Sustainable Energy

($\frac{X}{H_c}$) required to avoid collector shadowed at solar-noon for the winter solstice as a function of collector tilted angle and latitude angle. This means that the shaded zone length ratio ($\frac{Z_1}{X}$) is equal to the distance ratio ($\frac{X}{H_c}$) at this case.

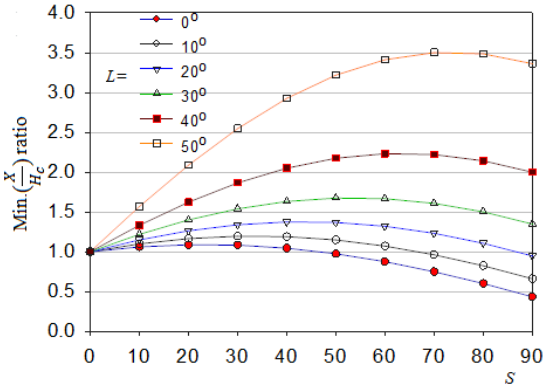

Fig. 3. Minimum ($\frac{X}{H_c}$) ratio required to avoid collector shadowed at solar-noon for winter solstice vs. tilt angles for several latitudes.

In general, for all latitudes increasing the tilt angle causes increasing in the view factor $F_{A2\to Z1}$ as a reaction for increasing the shadow zone with respect to the solar altitude angle to a certain critical tilt angle as it presented in fig.3. The sharp increasing in the value of $F_{A2\to Z1}$ is decaying by moving upward to high latitudes. As an exclusive from this rule, for low latitudes down Cancer tropic when ($\alpha > S$) still there is a shaded zone. The shaded zone is decaying from ($\alpha = 90°$) until again ($\alpha = S$) this cause decreasing of view factor. Of course the view factor $F_{A2\to Z1}$ decreases with spend days ahead to the summer solstices. The reason for that is the decay of the shaded zone during this journey, and vice versa occurs during the return trip from the summer to the winter solstice.

Increasing the tilt angle causes an increase in the value of $F_{A2\to Z2}$. This tendency is accelerated rapidly when moving upwards towards higher latitudes.

Fig.4 presents the relationship between the irradiance ratio and the solar collector tilted angle at the minimum distance ratio ($\frac{X}{H_c}$). It is obvious that the irradiance ratio has an inversely proportional relationship with the surface tilted angle (S), thereby demonstrating the weight of the sky view factor ($F_{A2\to s}$). Analysis of fig.4 reveals that the variation of the solar radiation ratio is clear during the days associated with high tilt angles. This will occur especially in high latitudes, because collectors in solar fields are often tilted to the equator with angles equal to the latitude angle.

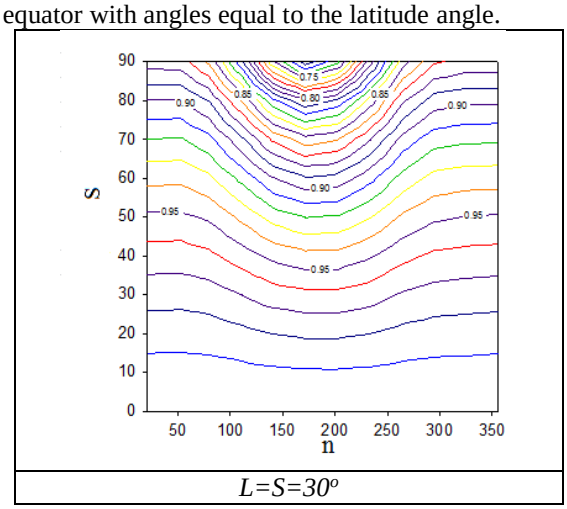

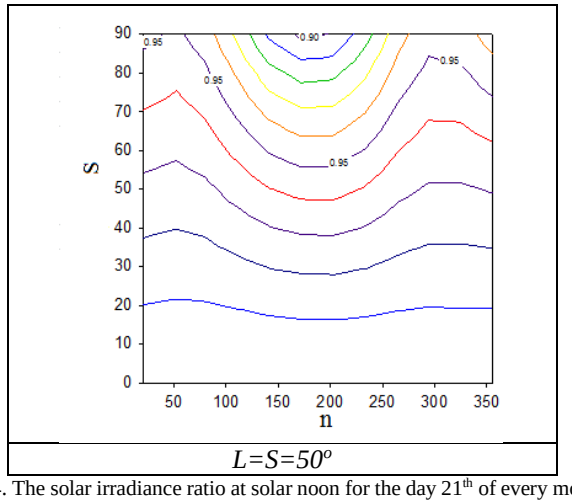

Fig.4. The solar irradiance ratio at solar noon for the day 21th of every month vs. the tilt angle (S) for various latitudes (L) according to the minimum ($\frac{X}{H_c}$) ratio associate with (S) and (L).

Determination of distance ratio ($\frac{X}{H_c}$) is very sensitive from both energetic and economic point of views. The capital cost of the land is a critical parameter. From one hand, increasing the distance ratio ($\frac{X}{H_c}$) results in an increase in the yield of the solar field. On the other hand, it is also increasing the capital cost. Therefore, it must reach a compromise between the growth of the yield as a result of increasing the distance ratio ($\frac{X}{H_c}$) and the rise of the capital cost due to increasing the land area. Fig.5 illustrates the effect of the distance ratio ($\frac{X}{H_c}$) on the solar irradiance ratio at solar noon for various latitudes while the tilt angle equals the latitude angle.

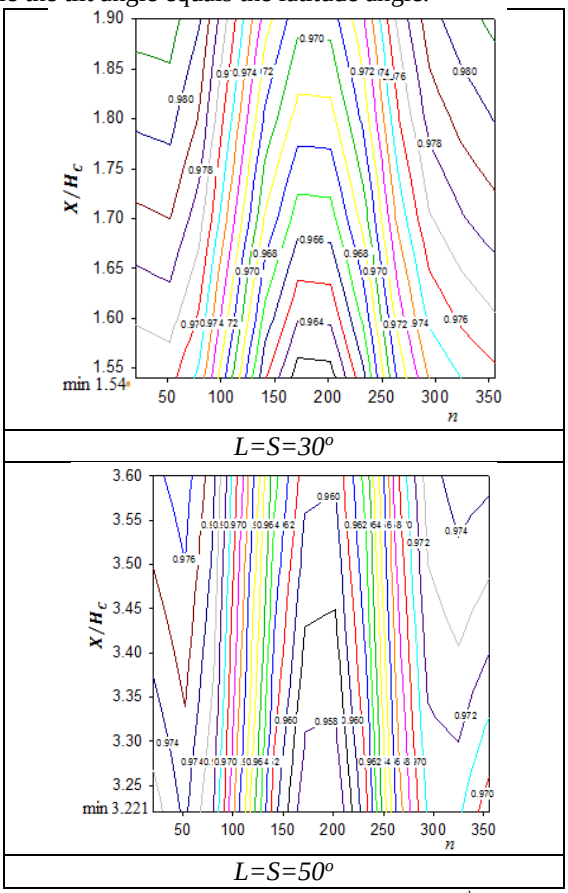

Fig.5. The solar irradiance ratio at solar noon for the day 21th of every month vs. the distance ratio ($\frac{X}{H_c}$) for various latitudes (L).

This article has been accepted for publication in a future issue of this journal, but has not been fully edited. Content may change prior to final publication. Citation information: DOI 10.1109/TSTE.2017.2697913, IEEE Transactions on Sustainable Energy

As expected, increasing the ratio ($\frac{X}{H_c}$), by increasing the distance separating the rows, or decreasing the collector height leads to an increase in the solar irradiance ratio. This increase is due to the growth in both the sky and ground view factors. The change in behaviour with the days is related to the position of the sun in the sky.

B. Experimental approach results

A non-published experimental investigation established early at May 2015 had been conducted on the measurement of solar irradiance incident on the second row of a prototype solar field built in Engineering Faculty, Brack-Libya, as presented schematically in fig.6. Unfortunately, the experiment was halted due to deficits in the equipment. The aim of this experiment is to illustrate the effect of the dimensions of the solar field on the electrical characteristics of the PV solar panels, enabling us to better understand the behaviour of PV solar panels in multi-rows solar fields. To show the reality of the present research, we provide fig.7, which is depicted and fitted by MATLAB Program, and it presents the degradation of the solar irradiance toward the centre of the row (which is not included in this research) and - of our interest - the effect of the distance separating ratio $\frac{X}{H_c}$ on the solar radiation, and down the fitting of these data. It is presented as a polynomial of 15 terms with 5th order in x and 2nd order in y. Where: f(x,y): presents I_f/I_t, x: presents X/H_c and y: presents $Y/(0.5L_c)$, L_c is the length of the row and Y is the location of the PV panel's centre from the row midpoint toward the edge of the row.

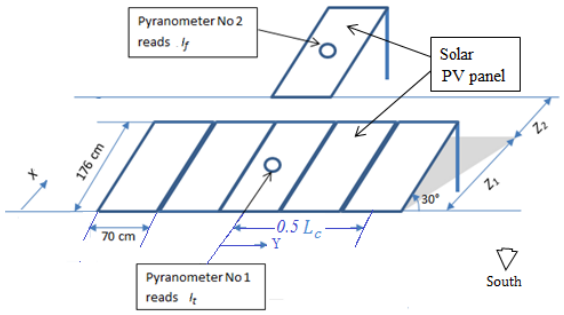

Fig.6. Layout of the experiment

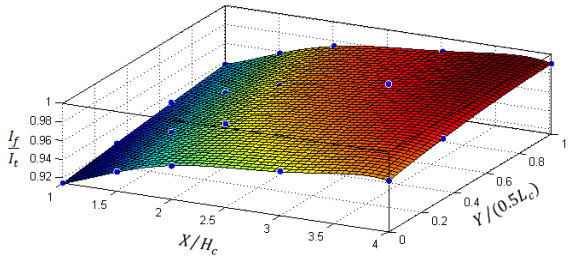

Linear model Poly52:
f(x,y) = p00 + p10*x + p01*y + p20*x^2 + p11*x*y + p02*y^2 + p30*x^3 + p21*x^2*y + p12*x*y^2 + p40*x^4 + p31*x^3*y + p22*x^2*y^2 + p50*x^5 + p41*x^4*y + p32*x^3*y^2
Coefficients (with 95% confidence bounds):
p00 =1, p10 =-0.3151, p01 =0.06783, p20 = 0.3743,
p11 =-0.07655, p02 =-0.03709,p30 = -0.1807,
p21 =0.03985, p12 =0.06124, p40 =0.03963,
p31 =-0.005831, p22 =-0.03146, p50 =-0.003259,
p41 = 3.662e-005, p32 = 0.004382.
Goodness of fit:
SSE:2.306e-5,R-square: 0.9994, RMSE: 0.0005739

Fig.7. The relation-ship between the (I_f/I_t) and the solar field design parameters (X/H_c, $Y/(0.5L_c)$) and the polynomial that fits the experimental data.

We tested all the possible compositions of the ratio (I_f/I_t) and found that the best estimation of the ratio (I_f/I_t), is included a composition of two models. The denominator which presents the total solar radiation on a single surface is one of the four models without any modification (Isotropic, Hay&Davies, Reindl and Perez), but the numerator must always be the isotropic model with modified view factor that is presented in eqn. (12). A comparison of using the isotropic, Hay/Davies, Reindl and Perez models in the denominator of the ratio with the experimental results is provided in fig.8. The experimental results have been provided in two measurement locations at the centre (y=0) and at the edge (y=1) of the row and also the average of the four measurements points (y=0, 1/3, 2/3, 1).

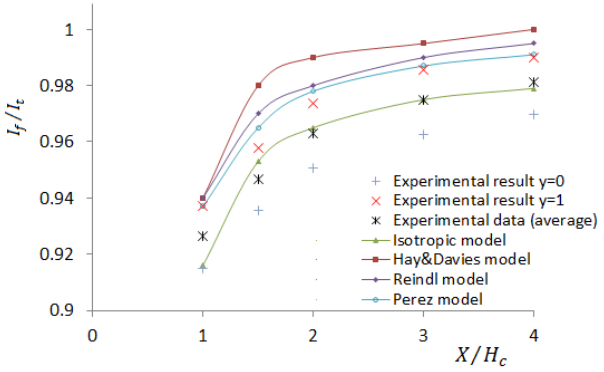

Fig.8. Comparison of analytical models to Measured data for solar irradiance on a solar field. y in the legend presents $Y/(0.5L_c)$)

It is obvious from fig.8 that the isotropic model is better representing the experimental results than the others models. The isotropic model achieves a satisfied identification with the average of experimental data, while the Perez model achieves best convergence with the row's edge measurement.

V. The Impact of Solar Radiation Degradation on PV Output Power

Considering the degradation of solar intensity on a PV panel as a partial shading, it is a well-documented fact that partial shading of a photovoltaic array reduces it output power capability. However, the relative amount of such degradation in energy production cannot be determined in a straight forward manner, as it is often not proportional to the shaded area. Many researches clarify the mechanism of partial PV shading on a number of PV cells connected in series and/or parallel with and without bypass diodes. Authors of [13] provided a simple analysis and can be useful to someone who wishes to determine the impact of some shading geometry on a PV system. The configuration considers two rows connecting in parallel and in series with diodes connecting in parallel with each row as it illustrated in fig. 9. The solar radiation intensity is considered uniform on the first row and non-homogenous along the second row.

This article has been accepted for publication in a future issue of this journal, but has not been fully edited. Content may change prior to final publication. Citation information: DOI 10.1109/TSTE.2017.2697913, IEEE Transactions on Sustainable Energy

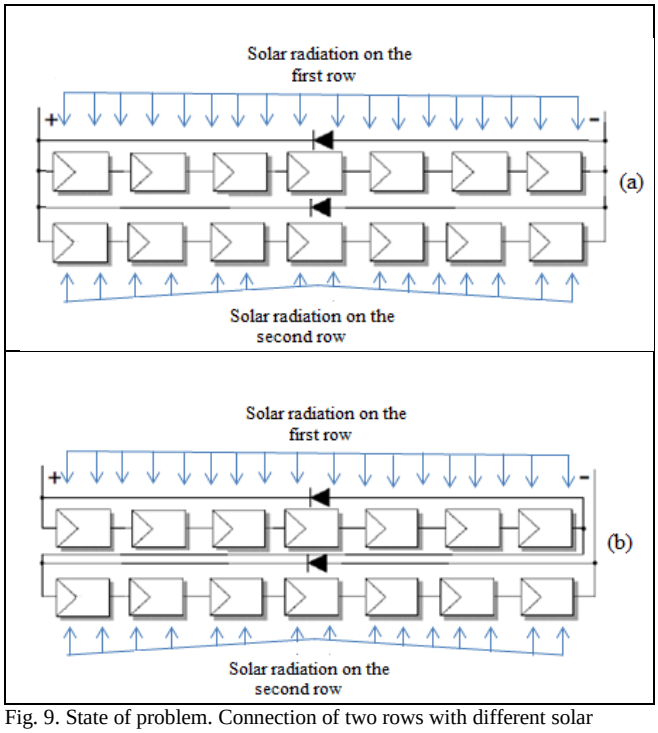

Fig. 9. State of problem. Connection of two rows with different solar intensity distribution with bypass diode in parallel with the rows (a) parallel connection and (b) series connection.

The resulting I-V characteristics of these configurations and the corresponding P-V curves for the above two cases, in addition to the case with uniform solar distribution on both rows are schematically shown in fig. 10(a, b).

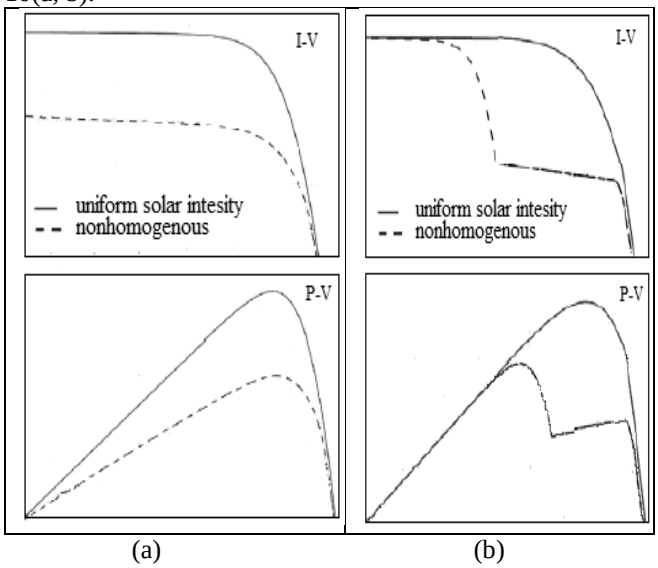

(a) (b)

Fig. 10. I-V characteristic and P-V of two rows with different solar irradiance intensities: (a) connected in parallel, and (b) connected in series.

Alternatively, when two rows with different irradiation intensities are connected together, the relative difference of their maximum power point (MPP) currents is much larger than the relative difference of their MPP voltages. This is due to the fact that the cell output current shows a stronger dependency (linear) on irradiation than the voltage (logarithmic). Therefore, in case of the series connection, if one row is working at its MPP, the other row having the same current works far from its MPP. The opposite is true in the parallel connection (i.e., if one row is working at its MPP, the other one sharing the same voltage will work also in the vicinity of its MPP, thus resulting in a higher MPP power) [14].

In solar fields there are many equipment that work as well as solar panels including MMP tracers, transformers and inverters, all these devices have unique electrical characteristics, thus further work must be conducted to estimate the yearly energy reduction due to the nonhomogeneous solar intensity on the solar field.

VI. Conclusions and Future Plans

The experimental results show that the second row of the solar field receives solar irradiation less than the first one. Furthermore, there is a degradation in solar intensity in the row directing towards the row's centre. The isotropic model is fairly represented the solar irradiance in the solar field with the average measurements data.

The proposed method makes it possible to estimate the hourly solar irradiance incident on a solar field and visualize the prospects of solar fields. The influence of the design parameters are analysed. This study shows that the tilt angle has an influential weight among all other design parameters, especially, in high latitudes. The tilt angle has been controlled in order to receive high solar irradiance. It records an effect of the time in the process; it is more sensitive in high latitudes and is associated with high tilt angles.

Therefore, it can be stated that the proposed model is perfectly applicable to any site where ordinary solar radiation information is available or predictable. Furthermore, it is comprehensive and generally able to consider any other configurations, such as an inclined plane or step-like structure solar fields, roofs, or facades of buildings. It only requires defining the view factors between the PV panels and the environment.

In order to illustrate the effect of solar intensity degradation on the performance of the PV solar fields, an intensive experimental investigation must be conducted on measurements the local and overall electrical characteristics of PV panel row under real situations of load and climatic conditions and for a long period of time.

References

[1] Geoffrey T. Klise and Joshua S. Stein, "Models Used to Assess the Performance of Photovoltaic Systems," SANDIA REPORT, SAND20092-8258, Dec. 2009.

[2] Matthew Lave, William Hayes, Andrew Pohl, and Clifford W. Hansen, "Evaluation of Global Horizontal Irradiance to Plane-of-Array Irradiance Models at Locations Across the United States," *IEEE journal of photovoltaics*, vol. 5, no. 2, pp. 597-606, Mar. 2015.

[3] Duffie, J. A. and Beckman, W. A., "Solar engineering of thermal process," 3rd ed., New York: John Wiley & Sons inc., 2006, pp. 96-101.

[4] Nasser, Y. F., "Solar energy engineering," Sebha University, Libya, 2006, pp. 51-102.

[5] W. De Soto, S.A. Klein, W.A. Beckman, "Improvement and validation of a model for photovoltaic array performance," *Solar Energy* 80, pp. 78–88, 2006..

[6] FK Tuffner, JL Hammerstrom, R Singh, "Incorporation of NREL Solar Advisor Model Photovoltaic Capabilities with GridLAB-D," the National Technical Information Service, U.S. Department of Commerce, 5285 Port Royal Rd., Springfield, VA 22161, Oct. 2012.

[7] Christopher P., Cameron C. P., W. E. Boyson, D. M. Riley, 2008, Comparison of PV System Performance-

Model Predictions with Measured PV System Performance, 33rd IEEE PVSC, San Diego, CA, May 12-16. Available: https://www.nrel.gov/ analysis /sam /pdfs /2008_sandia_ieee_pvsc.pdf

[8] Solar Collectors and Photovoltaic in energyPRO with array shading, Sep. 2013. Available: www.emd.dk.

[9] J. Appelbaum, "Current mismatch in PV panels resulting from different locations of cells in the panel," *Solar Energy* 126, pp. 264–275, 2016.

[10] J. Appelbaum and A. Aronescu, "View factors of photovoltaic collectors on Roof Tops," *Journal of Renewable and Sustainable Energy* 8, 2016.

[11] Nassar Y.F. and Alsadi S., "View factors of flat solar collectors array in flat, inclined, and step-like solar fields," *Journal of Solar Energy Engineering, ASME Tran.*, vol. 138, pp. 1-8, 2016.

[12] S. Alsadi and Y. Nassar, "Correction of the ASHRAE clear-sky model parameters based on solar radiation measurements in the Arabic countries," *International Journal of Renewable Energy Technology Research*, vol. 5, no. 4, pp. 1-16, July 2016.

[13] Y. Sun, S. Chen, L. Xie, R. Hong, and H. Shen, "Investigation the impact of shading effect on the characteristics of a large-scale frid-connected PV power plant in Northwest China," *International Journal of Photoenergy*, volume 2014, pp1-9, 2014. available: http://dx.doi.org/10.1155/2014/763106

[14] Sera, D., and Baghzouz, Y., "On the impact of partial shading on PV output power," in proceedings of RES'08 ESEAS Press. 2008. Available: http://vbn.aau. dk/files/17328065/

Samer Yassin Alsadi: An Associate Professor received the PhD degree in electrical power engineering from Moscow Power Engineering Institute (Technical University), Moscow, Russia, in 2000.

He worked as a Consultant in Electrical Department of city's municipality for one year, and since 2001, he has been working at Palestine Technical University-Kadoorie-Tulkarm, in the department of Electrical Engineering. His research interests focus on solar energy, power systems, protection systems, load forecasting.

Yasser Fathi Nassar: A Professor received the B.Sc. degree in power mechanical engineering from Tripoli University in 1990, M.Sc. and PhD in solar energy systems from Moscow Power Engineering Institute (Technical University), Moscow-Russia, in 1999. Since 2000, he is a lecturer in mechanical engineering department, Faculty of engineering and technology, Sebha university-Libya. His research interests include PV/T solar collectors, modelling and optimization processes of solar system.